A Comparison of Methods for the Analysis of Wing-Tail Interaction Flutter

WILLIAM E. TRIPLETT,* THOMAS H. BURKHART,† AND EDWIN B. BIRCHFIELD†
McDonnell Aircraft Company, St. Louis, Mo.

Results of an analytical investigation of the aeroelastic stability of variable sweep aircraft, specifically with respect to wing-tail interaction flutter, are presented. Three aerodynamic representations are employed: 1) modified two-dimensional strip theory containing no wing-tail aerodynamic interaction, 2) vortex lattice theory containing aerodynamic interaction of wing on tail only, and 3) subsonic kernel function theory containing a complete evaluation of wing-tail aerodynamic interaction. The capability of the interaction methods is established by an application to an experimental flutter model where wing-tail aerodynamic interaction is known to be of importance. The aerodynamic methods are then applied to a particular high performance variable sweep aircraft. The basic flutter mechanisms for this hypothetical aircraft are generated by wing-fuselage mechanical interaction and are predicted by wing aerodynamics alone. Component aerodynamics on wing and tail without interaction do not predict the mechanism. Aerodynamic interaction causes the reappearance of flutter at a velocity 30% lower than generated by the wing alone.

Introduction

ANALYTICAL and experimental investigations concerned with the aeroelastic stability of variable sweep aircraft have indicated flutter mechanisms which involve the entire airframe. These flutter mechanisms combine the vibratory behavior of the wing with that of the fuselage and tail. When the wing is in close proximity to the tail, the aerodynamic interaction of the wing-tail system can significantly affect the aeroelastic stability of the aircraft. Experimental investigations reported in Ref. 1 indicated a dramatic flutter speed degradation with the variable sweep wing in the most aft position. Theoretical analyses of Ref. 1 using three-dimensional generalized forces computed for each surface with no aerodynamic interaction failed to predict the wing-tail flutter mechanism. Additional experimental data were reported in Ref. 2 which indicated destructive flutter for an elementary variable sweep flutter model, and an analytical method was presented which was able to predict the flutter instability by evaluating the aerodynamic influence of the wing on the tail by a vortex lattice procedure. Analytical investigations presented in Ref. 3 using a linear potential flow aerodynamic theory representing complete wing-tail aerodynamic interaction predicted the wing-tail interaction flutter for the model of Ref. 1 and indicated that the instability was not predicted if the aerodynamic interaction between the component surfaces was suppressed. Flutter analyses and wind tunnel tests reported in Ref. 4 give conclusive proof that interaction aerodynamics between wing and tail is an important and detrimental effect.

This paper presents results of an analytical investigation of the aeroelastic stability of a high performance variable sweep aircraft shown in Fig. 1, specifically in regard to wing-tail interaction flutter. The principal purpose of the analytical effort was to obtain the highest degree of confidence possible regarding the flutter stability of this advanced aircraft. Three separate aerodynamic representations were used to accomplish this objective. These methods were 1) modified two-dimensional strip theory containing no aerodynamic interaction, 2) vortex lattice lifting surface theory providing for the aerodynamic influence of the wing on the tail, and 3) subsonic kernel function theory containing a complete potential flow representation of the aerodynamic interaction of the wing-tail system. The validity of the methods was first established by application to the experimental flutter model of Ref. 2 where wing-tail interaction was known to be of importance. The three methods were then applied to the advanced aircraft. These investigations served not only to increase the confidence concerning the flutter stability of the advanced aircraft as intended, but also produced significant results concerning the basic nature of the wing-tail flutter mechanisms.

Presented as Paper 70-80 at the AIAA 8th Aerospace Sciences Meeting, New York, January 19–21, 1970; submitted February 17, 1970; revision received October 22, 1970.

* Technical Specialist, Structural Dynamics. Member AIAA.
† Senior Engineer, Structural Dynamics.

Aerodynamic Methods

The three separate aerodynamic methods considered are modified strip theory, vortex lattice theory, and kernel function theory.

Modified Strip Theory

The modified strip theory is similar to that presented in Ref. 5. It is based on classical two-dimensional potential flow theory in which the circulatory components of the aerodynamic forces are corrected for finite aspect ratio and com-

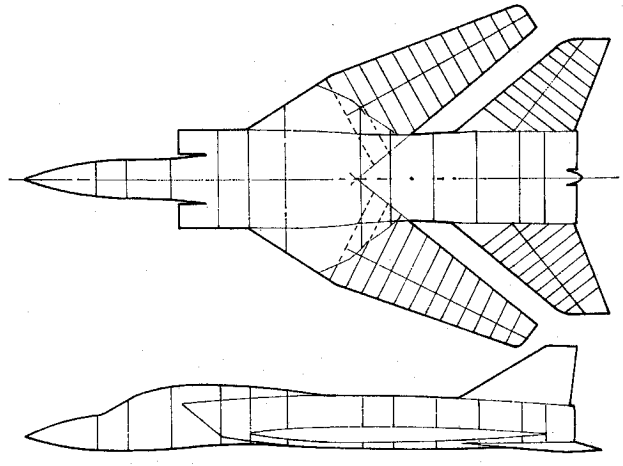

Fig. 1 Aircraft structural idealization.

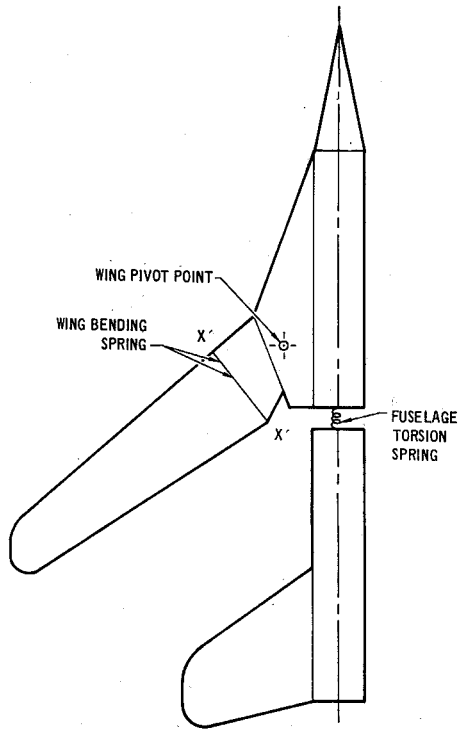

VIBRATION MODE DESCRIPTION	FREQUENCY – HERTZ	
	40° WING SWEEP	70° WING SWEEP
1ST CANTILEVER WING BENDING	5.19	5.55
CANTILEVER AFT FUSELAGE TORSION	7.14	7.14

Fig. 2 Wing-tail flutter model planform view.

pressibility effects. Corrections are based on static wind tunnel data. Aerodynamic forces are obtained for the wing only; that is, no tail or interaction aerodynamics are included.

Vortex Lattice Method

The vortex lattice method is the same as that presented by Shelton, Tucker, and Davis in Ref. 2. This method considers the aerodynamic interaction effect of the wing on the tail but not the effect of the tail on the wing. The method includes some effects not found in the purely linear theories. These special features of the method are that 1) the deflection of the trailing vortex sheet resulting from the static lift of the aircraft is computed and 2) the variation in downwash on the tail resulting from oscillating motion of the tail relative to the mean trailing vortex sheet is included in evaluation of the tail loading.

The evaluation of the aerodynamic forces is initiated by computing the static aerodynamic loading on the wing and tail individually for each vibration mode shape. This is performed using the three-dimensional subsonic vortex lattice theory as given in Ref. 6. Unsteady correction factors are applied to these load distributions using compressible finite aspect ratio indicial lift growth functions. The resulting unsteady aerodynamic loads are used to evaluate the "circulatory generalized forces" to which are added noncirculatory generalized forces to account for apparent mass effects. These noncirculatory forces are based on two-dimensional potential flow theory with modifications for finite aspect ratio. The induced downwash on the tail caused by loading on the wing is evaluated by replacing the wing loading with a horseshoe vortex system and defining the downwash at a point on the tail by the Biot-Savart Law. The first step is to calculate the static position of the trailing vortex sheet caused by the static lift of the aircraft, including the effects of deformation of wing and tail resulting from the static lift. Then the induced downwash on the tail is evaluated considering two effects: 1) the variation of wing lift caused by generalized coordinate motion of the wing, and 2) the generalized coordinate motion of the tail relative to the static position of the trailing vortex sheet. The static loading of the tail caused by this induced downwash is obtained by applying once again the vortex lattice procedure. Unsteady effects are applied to the induced tail loading using a combination of "transport lag" and "lift growth" functions. The generalized forces resulting from this unsteady induced tail loading are evaluated and added to the previously defined set of generalized forces to complete the calculations.

Kernel Function Method

The subsonic kernel function method, described in detail in Ref. 7, is based on linearized subsonic three-dimensional potential flow theory. This method, when applied to wing-tail configurations, includes the complete aerodynamic interaction between the wing and tail. It simultaneously considers both vibratory and induced downwashes when evaluating the oscillatory loading on the wing and tail and all unsteady and compressibility effects are explicitly included.

The evaluation of the aerodynamic loading is performed by obtaining a collocation solution to the integral equation relating the oscillatory downwash at a point to the aerodynamic loading which is expressed by the following:

$$W(x,s) = \sum_{\nu=1}^{2} \iint \Delta p_\nu(\zeta,\sigma) K(x-\zeta, s-\sigma)\, d\zeta\, d\sigma$$

nth surface; νth surface

where x and ζ are streamwise coordinates, s and σ are spanwise surface coordinates, and Δp_ν is the aerodynamic loading of the νth surface. W is the oscillatory downwash of the nth surface, and K the subsonic nonplanar kernel function. This approach is basically similar to that presented in Refs. 8, 9, and 10 with the exception that now the downwash at a point on one of the surfaces affects loading on both wing and tail.

To obtain the solution the aerodynamic loading is assumed to be composed of selected pressure modes whose weight factor coefficients are to be determined. The pressure modes used are of the form recommended in Ref. 8. The locations

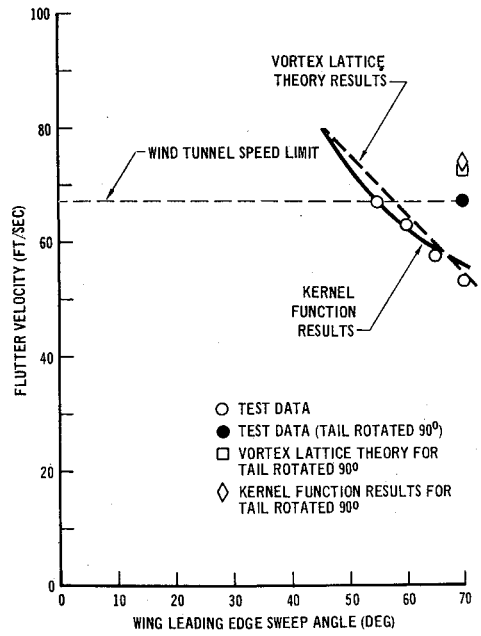

Fig. 3 Comparison of measured and calculated flutter velocity for flutter model.

of the collocation point stations are computed using formulas which have been proven to be optimum in Ref. 9. Evaluation of the above integral with respect to each collocation point and pressure mode coefficient is performed using a Gauss quadrature procedure similar to that presented in Ref. 10. The spanwise singularity is likewise handled using the procedures of Ref. 10. Convergence of the numerical integration and collocation point-pressure mode selection was found to be adequate with respect to the recommendations of Ref. 8.

Since the wing and tail of the configuration of interest are not coplanar, a nonplanar version of the kernel function was employed. The formulation of the kernel function is similar to that given in Ref. 11 for incompressible flow. The extension of this formulation to compressible flow was performed by Widnall along with procedures for numerical evaluation. The result of the numerical procedures is a complex matrix equation relating the oscillatory downwash at a set of collocation points on the wing and tail to a set of unknown pressure mode coefficients for the wing and tail loading. Evaluation of the coefficients is performed by matrix operations and these coefficients are then used to evaluate numerically the generalized aerodynamic forces.

Results

Verification of Methods with Test Results

To assess the capability of the three-dimensional aerodynamic methods, they were applied to the low speed flutter model of Ref. 2. This model, shown in Fig. 2, simulates the primary modes of interest in antisymmetric wing-tail interaction flutter: wing bending, fuselage torsion and rigid body roll. The horizontal tail is attached to and moves with the aft fuselage. Pitch rotations of the tail are not allowed. The component flutter speed of the tail is well beyond the range of the tunnel. The wing is relatively stiff outboard of the bending spring to preclude component wing flutter. Vibration data for the model are also shown in Fig. 2.

Test results for this flutter model were originally presented in Ref. 2 and are shown in Fig. 3. The effect of wing-tail aerodynamic interaction was evaluated by testing the model both with a coplanar wing-tail arrangement and with the tail rotated 90° from the wing plane. This provided data for the model both with and without aerodynamic interaction for the same model dynamics.

Analytical results for both the kernel function and vortex lattice methods applied to the model are shown in Fig. 3. These results were obtained by classical velocity vs damping solution techniques. They show similar trends for the coplanar wing-tail arrangement, and the maximum deviation from a corresponding experimental flutter speed is less than 4% for both of the methods. The analytical results for both methods are within 1% of each other and about 10% higher than the experimental result for the noninteractive case of the orthogonal wing-tail arrangement. Analytically, about a 27% drop in the flutter speed is predicted because of aerodynamic interaction, whereas the experimental drop is only 22%.

Based on this comparison with experiment, it may be concluded that the vortex lattice and kernel function methods are both adequate in predicting the flutter speed of this type of configuration with or without aerodynamic interaction. The vortex lattice method does not include the tail-to-wing aerodynamic interaction; thus, the minor differences between the two methods for the coplanar case indicate the relative insignificance of this upstream interaction.

Application of Methods to Aircraft Configuration

The major results reported in this paper are from analyses of the particular aircraft shown in Fig. 1 using the three separate aerodynamic methods. Extensive analyses were first made by the modified two-dimensional strip theory method to establish flutter trends for both the wing and horizontal tail. Detailed analyses by the kernel function and vortex lattice theories were then performed to provide better quantitative data.

Basic vibration data

A set of normal modes were calculated for the fuselage, wing and horizontal tail and used as basic data for each of the flutter analyses. Beam-rod analogies were used as the basic structural idealization for each of the primary components. Classical eigenvalue techniques were used in computing the natural vibration mode shapes and frequencies. The idealization for the particular aircraft presented in this paper is shown in Fig. 1. The wing is represented by 12 discrete uniform rigid chord sections and the horizontal tail by 10 such sections. The fuselage is cut into 13 nonuniform sections. All sections are normal to assumed elastic axes.

In order to simplify the determination of the wing dynamic characteristics with variable sweep, the wing elastic properties are described in two parts. One part is inboard of the pivot and is described by a set of influence coefficients relating deflections and forces at the wing pivot point. The other part is outboard of the pivot and is represented as being cantilevered from the wing pivot point. These two parts are combined, for any desired sweep angle, by use of an orthogonal transformation at the wing pivot point. For the modified strip theory analyses the wing mode shapes are evaluated to give rigid streamwise chords. However, in both the vortex lattice and kernel function analyses the mode shapes are evaluated to give the induced camber in the streamwise direction because of sweep angle.

The horizontal tail structural modes are cantilevered from the point where the actuator hinge line intersects the root-rib. The rigid pitch rotation of the tail about the hinge line is considered as a separate generalized coordinate.

The fuselage torsion modes are calculated for the free-free case. The rolling inertia of the entire aircraft about the centerline, including the rigid wing and tail surfaces, is used in the torsion mode calculations.

The vibration frequencies and a description of the predominant characteristic of each vibration mode considered in the study are shown in Table 1 for three wing sweep positions. Only the antisymmetrical structural modes are tabulated since for this particular aircraft no wing-fuselage or wing-tail flutter mechanisms exist for symmetrical aircraft motion.

The fuselage modes are for a fully loaded configuration and reflect the relatively high rolling moment of inertia of the wide fuselage. Small changes caused by the decrease in rolling moment of inertia of the wing with wing sweep, about the aircraft center line, are indicated. The wing vibration modes vary with sweep angle as a result of the relative values of the pitch and roll influence coefficients at the wing pivot. The root (or pivot) stiffness is greater in pitch than it is in roll; therefore, wing bending frequencies increase and wing torsion frequencies decrease with wing sweep angle.

Results for rigid horizontal tail

Flutter analyses of the aircraft configuration of Fig. 1 were made early in the design cycle using an antisymmetrical 8 degree of freedom dynamic representation. These degrees of freedom were the five lowest wing modes, the two lowest fuselage torsion modes, and the rigid aircraft roll mode. The tail was considered structurally rigid and rigidly attached to the aft fuselage. Because of the relative locations of the actuator support point and hinge line, the rigid tail experiences an angle of attack caused by the fuselage torsion modes.

Modified two-dimensional strip theory was used to establish flutter trends. The flutter boundary variation with

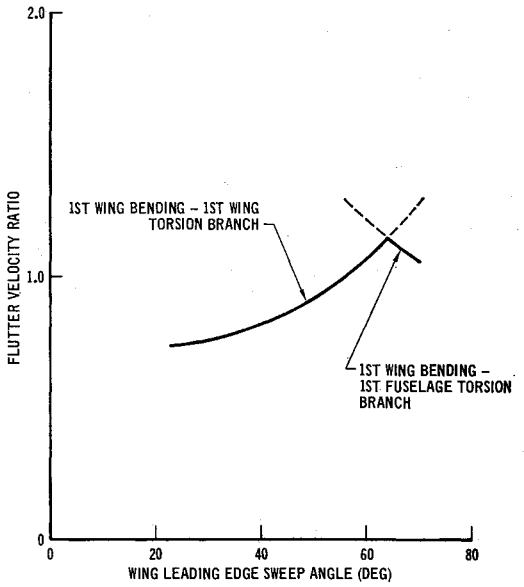

Fig. 4 Flutter velocity vs sweep angle—modified strip theory —rigid horizontal tail.

wing sweep angle is shown in Fig. 4. The strip theory method predicts the typical and expected increases in the wing bending–wing torsion flutter velocity with increasing sweep angle up to about 65°. For greater sweep angles, the critical flutter mode is no longer wing bending-wing torsion, but an instability involving coupling of wing bending with fuselage torsion. Since the strip theory results contain no tail or interaction aerodynamics, this change in flutter mechanism is a direct result of the variation of the system dynamics with sweep angle.

Parametric studies for the most aft sweep position were performed to further investigate the wing bending-fuselage torsion flutter mechanism by varying the frequency ratio of these two critical modes. These parametric studies were performed using strip theory, kernel function theory, and the vortex lattice method for a Mach number of 0.9. Figure 5

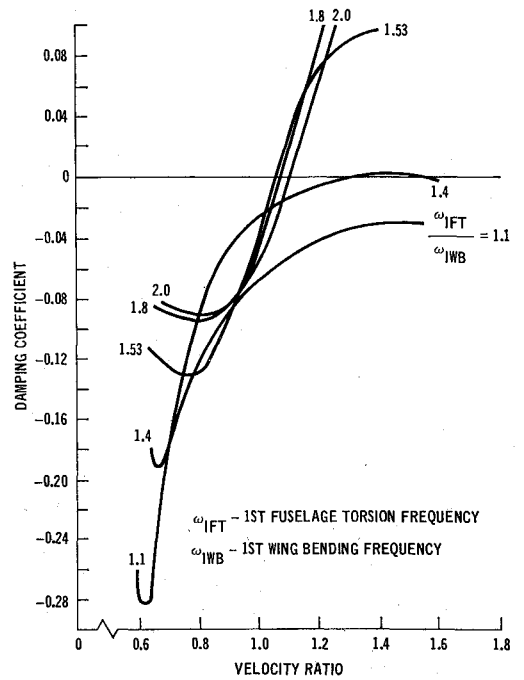

Fig. 5 Damping coefficient vs velocity ratio for variation of first fuselage torsion to first wing bending frequency ratio—modified strip theory—rigid horizontal tail.

shows the results of the strip theory studies with a classical plot of damping required for stability vs velocity. Figure 6 presents similar results for the kernel function method. The results from both methods indicate similar characteristics. For frequency ratios less than 1.4, the flutter mechanism does not go unstable, although its essential character is still apparent. For frequency ratios greater than 1.4, the flutter crossings are relatively steep.

Figure 7 compares the damping vs velocity results from the three methods for a frequency ratio of 1.53. The kernel function method characteristically indicates the highest damping levels prior to instability with the strip theory result indicating the lowest. However, the flutter velocity crossings for these two methods are within 5%. The vortex lattice method indicates the lowest flutter velocity, 10% below the kernel function result.

The flutter boundaries, obtained by the three methods, are presented in Fig. 8 as a function of frequency ratio. Two separate flutter mechanisms are indicated: first wing bending coupled with first fuselage torsion, and first wing bending coupled with second fuselage torsion. The results of the three methods agree reasonably well for the wing bending-first fuselage torsion branch, while the comparison is less favorable for the wing bending-second fuselage torsion branch. Differences between the vortex lattice and kernel function results can be attributed to compromises in the vortex lattice analyses concerning the effective fuselage torsion modal slope at the wing pivot point. The wing carry-through structure for this aircraft is a rigid triangular box attached at two distinct points at the fuselage mold line. The forward attach point is a pinned joint which transmits shear only. The vortex lattice computer program analytically evaluates the slope of the fuselage torsion mode at the wing pivot point and does not consider the unique behavior of the rigid carry-through box structure. The kernel function and strip theory computer programs accept tabulated modal deflection data. The more appropriate effective slope of the fuselage torsion mode at the wing pivot point could thus be used with these two programs. Since only the second fuselage torsion mode was significantly affected and since this mode was not of primary importance for this aircraft, the vortex lattice analyses were not updated. The modified two-dimensional strip theory results are surprisingly close to the kernel function results for both branches of the flutter boundary.

Table 1 Aircraft vibration data

Vibration mode description	Vibration frequency (Hz) Wing sweep position 23°	45°	70°
Fuselage (free-free with rigid wing and tail)			
1st torsion	11.6	11.8	11.9
2nd torsion	20.5	20.6	20.8
3rd torsion	28.5	28.6	28.8
4th torsion	49.4	49.5	49.7
Wing (cantilevered from aircraft centerline)			
1st bending	7.0	7.4	7.8
2nd bending	21.0	21.5	22.3
1st torsion	32.4	31.1	29.8
3rd bending	42.4	42.8	43.0
2nd torsion	65.6	64.5	63.2
Horizontal tail (cantilevered from hingeline)			
1st bending		11.5	
2nd bending		32.5	
1st torsion		62.6	
3rd bending		77.5	
Rigid rotation (nominal)		20.0	

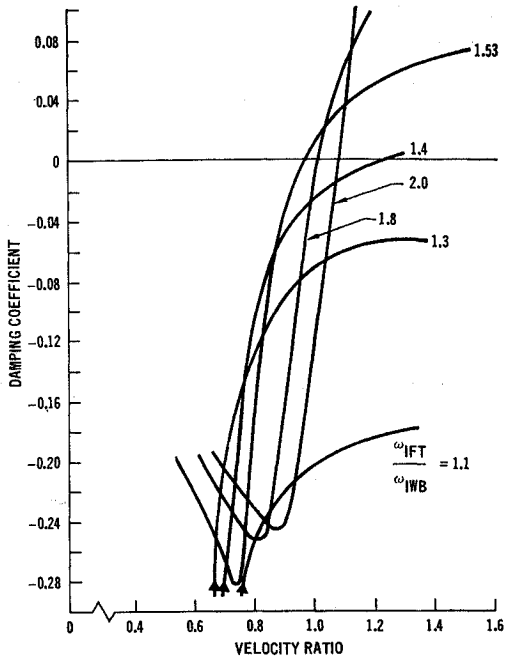

Fig. 6 Damping coefficient vs velocity ratio for variation of first fuselage torsion to first wing bending frequency ratio—kernel function method—rigid horizontal tail.

Additional studies were made by the kernel function method considering aerodynamic forces on the wing only, and on the wing and tail with no aerodynamic interaction. Figure 9 compares the flutter boundary for the studies performed with complete interaction aerodynamics and with wing aerodynamics only. The effect of the complete interaction aerodynamics was to lower the flutter speed 30% relative to the wing only results. The results using wing and tail aerodynamics without interaction did not show the first wing bending-fuselage torsion flutter mechanism. This behavior, which agrees with Refs. 1 and 3, is clarified in Fig. 10. For the case of wing aerodynamics only, the fuselage torsion mode is virtually unaffected by aerodynamic forces, and the wing bending mode, which increases with airspeed,

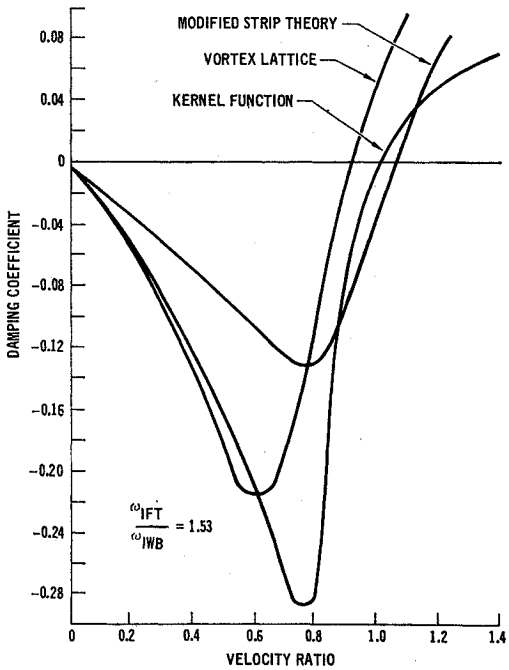

Fig. 7 Damping coefficient vs velocity ratio—comparison of three methods—rigid horizontal tail.

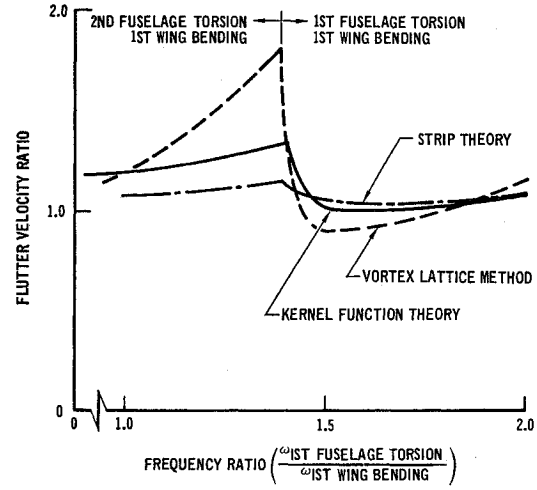

Fig. 8 Flutter velocity ratio vs first fuselage torsion to first wing bending frequency ratio—comparison of three methods—rigid horizontal tail.

coalesces with the torsion mode. The addition of the tail aerodynamics without interaction introduces aerodynamic forces which cause the fuselage torsion frequency to increase with air speed also, thus preventing coalescence. The further addition of interaction aerodynamics increases the cross coupling force between these degrees of freedom such that the flutter mechanism reappears and at a lower speed than predicted by the wing only case.

Results for elastic horizontal tail

Since the elastic tail could couple with the fuselage torsion mode, additional studies were conducted using a 15 degree of freedom representation. These degrees of freedom were the five lowest wing modes, the four lowest stabilator modes, the stabilator rigid body pitch rotation mode, the four lowest fuselage torsion modes, and the rigid aircraft roll mode. All of the 15 degree of freedom studies were made using the multiple surface kernel function method.

The flutter boundary for this system is plotted vs the stabilator rigid rotation frequency in Fig. 11. The flutter mechanism for stabilator rotation frequencies less than 18 Hz is the coupling of the stabilator rotation mode with the first fuselage torsion mode. For stabilator rotation frequencies of 18 Hz or greater the flutter boundary reverts to the first wing bending-first fuselage torsion flutter mechanism.

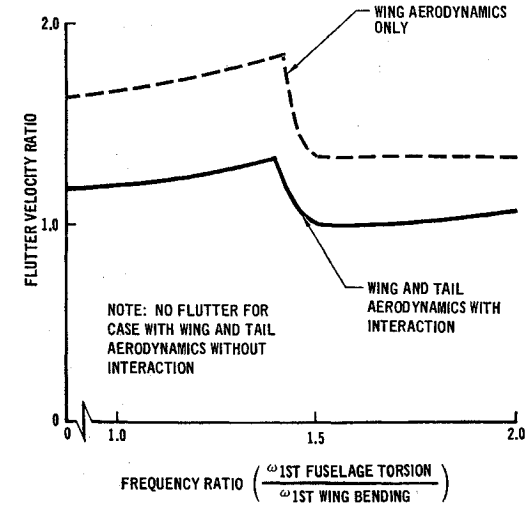

Fig. 9 Flutter velocity ratio vs first fuselage torsion to first wing bending frequency ratio—comparison of kernel function results.

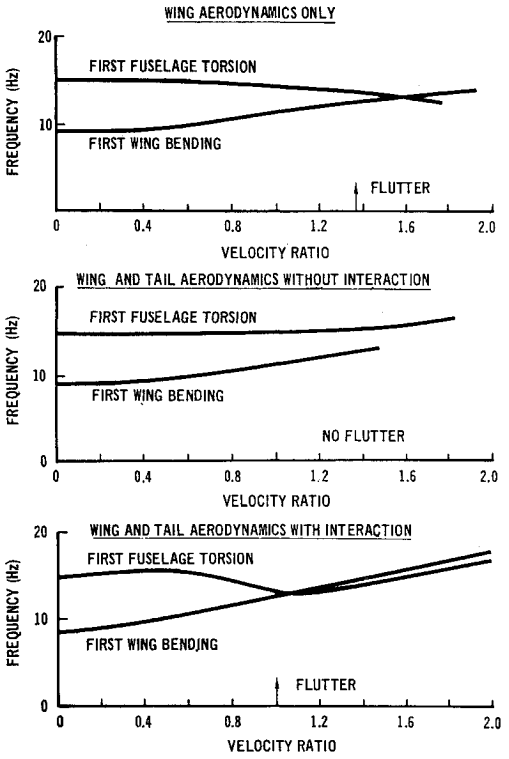

Fig. 10 Frequency vs velocity ratio—kernel function method—effect of interaction aerodynamics—rigid horizontal tail—$\omega_{1FT}/\omega_{1WB} = 1.53$.

Also shown on Fig. 11 are data points from an eight degree of freedom (two fuselage torsion, five stabilator, and rigid aircraft roll) modified two-dimensional strip theory analysis. Again, the strip theory not only shows expected trends but also shows surprisingly close agreement with the kernel function results. The implication is that the stabilator rotation-fuselage torsion mechanism is not a function of the wing modes or of the downwash created by the wing.

It is interesting to note that when the stabilator rotation-fuselage torsion mode is the critical flutter mode it eliminates

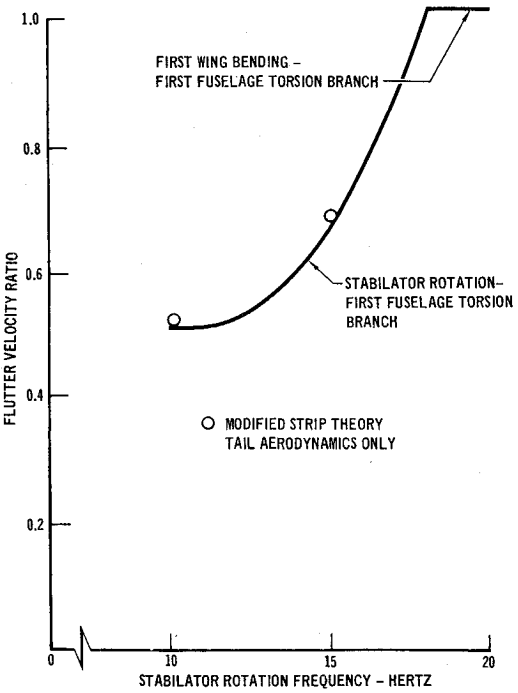

Fig. 11 Flutter velocity vs stabilator rotation frequency—kernel function method—elastic horizontal tail.

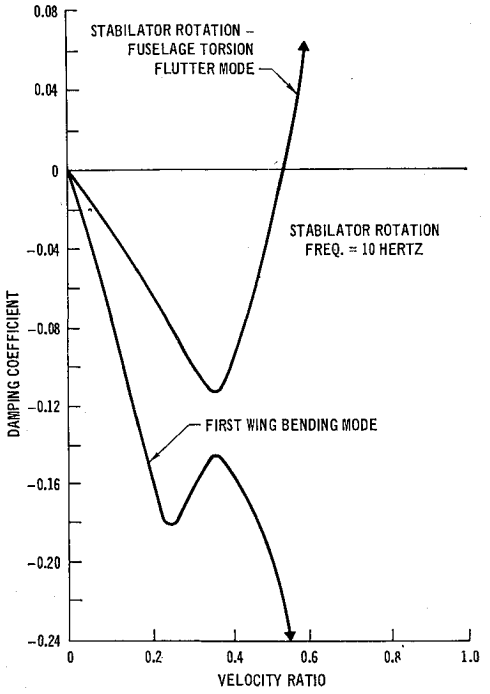

Fig. 12 Damping coefficient vs velocity ratio—kernel function method—elastic horizontal tail.

the wing bending-fuselage torsion mechanism. Results for the 15 degree of freedom kernel function study are presented in Fig. 12 by the classical damping vs velocity curves for a stabilator rotation frequency of 10 Hz. The first wing bending-first fuselage torsion mechanism is stable while the stabilator rotation-fuselage torsion mechanism is unstable. The stabilator rotation-fuselage torsion flutter mode stabilizes the wing bending-fuselage torsion mode by a modification of the fuselage mode. This situation holds for all values of fuselage torsion-wing bending frequency ratio. Similar results occur for any stabilator rotation frequency less than 18 Hz, that is for all cases where the stabilator provides an instability below the wing bending-fuselage torsion flutter speed.

The mechanism involving the stabilator rotation mode and the fuselage torsion mode stabilizes the wing bending-fuselage torsion flutter mechanism by modifying the characteristics of the fuselage torsion mode. The implication is that a potential wing-tail interaction instability involving the wing bending and fuselage torsion modes could be prevented by a modification of the fuselage torsion mode using the stabilator and a feedback control system. This should be considered when wing-tail instabilities are uncovered on existing aircraft or where the "control-configured vehicle" concept is used in the initial design.

Conclusions

The following conclusions can be drawn on the basis of the work presented here:

1) Although aerodynamic wing tail interaction has been shown to be a very important ingredient to the flutter stability of some aircraft, the critical flutter modes of this configuration involved primarily mechanical interaction, modified by aerodynamic interaction.

2) The effects of tail-to-wing aerodynamic interaction are practically negligible.

3) Modified strip theory provides a quite adequate means for quickly and inexpensively predicting the basic flutter trends of a configuration such as the one analyzed here at an early design stage. For increased confidence and improved accuracy, these analyses should be verified by one of the more

sophisticated theories which account for aerodynamic interaction. However, for configurations with lighter and thinner fuselages, it is believed that the aerodynamic interaction will prove to be more important, and such configurations will require early analysis with an accurate interaction aerodynamic theory.

4) For the successful prediction of the airframe critical flutter mode, the dynamic idealization must realistically include the elastic characteristics of all interactive components.

5) Complete aircraft flutter analyses using component aerodynamics without interaction (i.e., wing and tail aerodynamics separately) should be avoided because such analyses may obscure the potentially critical wing-tail mechanism.

6) A potential wing-tail interaction instability can be prevented by geometric rearrangement, or by considerable structural stiffening, and quite possibly by "active control" with the stabilator control system.

References

[1] Topp, L. J., Rowe, W. S., and Shattuck, A. W., "Aeroelastic Considerations in the Design of Variable Sweep Airplanes," ICAS Paper 66-12, 5th International Council of the Aeronautical Sciences Congress, London, 1966.

[2] Shelton, J. D., Tucker, P. B., and Davis, J. C., "Wing-Tail Interaction Flutter of Moderately Spaced Tandem Airfoils," AIAA Paper 69-57, New York, 1969.

[3] Sensburg, O. and Laschka, B., "Flutter Induced by Aerodynamic Interference Between Wing and Tail," *Journal of Aircraft*, Vol. 7, No. 4, July-Aug. 1970, pp. 319–324.

[4] Mykytow, W. J. et al., "Subsonic Flutter Characteristics of a Variable Sweep Wing and Horizontal Tail Combination," AFFDL-TR-69-59, 1969, Wright-Patterson Air Force Base, Ohio.

[5] Yates, E. C., Jr., "Modified Strip Analysis Method for Predicting Wing Flutter at Subsonic to Hypersonic Speeds," *Journal of Aircraft*, Vol. 3, No. 1, Jan.-Feb. 1966, pp. 25–29.

[6] Falkner, V. M., "The Calculation of Aerodynamic Loading on Surfaces of Any Shape," British RM 1910, 1943, National Physics Laboratory.

[7] "The Development of Subsonic Unsteady Aerodynamics for Wing-Tail Interference," Rept. G246, Vol. 3, May 1968, McDonnell Aircraft Co., St. Louis, Mo..

[8] Rowe, W., "Collocation Method for Calculating the Aerodynamic Pressure Distribution on a Lifting Surface Oscillating in Subsonic Compressible Flow," *AIAA Symposium on Structural Dynamics and Aeroelasticity*, Boston, 1965.

[9] Hsu, P., "Flutter of Low Aspect-Ratio Wings, Part I Calculation of Pressure Distributions for Oscillating Wings of Arbitrary Planform in Subsonic Flow by the Kernel Function Method," ASRL 64-1, 1957, M.I.T., Cambridge, Mass.

[10] Watkins, C. E., Woolston, D. S., and Cunningham, H. J., "A Systematic Kernel Function Procedure for Determining Aerodynamic Forces on Oscillating or Steady Finite Wings at Subsonic Speeds," TR R-48, 1959, NASA.

[11] Ashley, H., Widnall, S., and Landahl, M., "New Directions in Lifting Surface Theory," *AIAA Journal*, Vol. 3, No. 1, Jan. 1965, pp. 3–16.

MAY 1971 J. AIRCRAFT VOL. 8, NO. 5

Advanced Design Concepts for Buckling-Critical Composite Shell Structures

L. B. Greszczuk* and R. J. Miller†
McDonnell Douglas Astronautics Company, Santa Monica, Calif.

The high cost of advanced filamentary composites has led to the investigation and development of new design concepts for buckling-critical composite shell structures. Results are presented on structural efficiency and cost effectiveness of shells designed for buckling under external pressure and axial compression. Use of a pseudo-*T*-rib stiffening concept in which small quantities of high-modulus fibers are placed at the tip of a metal stiffener significantly increases buckling efficiency. A 10-volume-percent of boron-epoxy (as compared to the total volume of material in a stiffened metal shell) increases the buckling efficiency of an externally pressurized shell as much as 80% at a cost comparable to that of all-metal structures. Similar results are obtained for buckling-critical shells subjected to axial compression. For an integrated-composite shell consisting of an aluminum cylinder overwrapped with boron-epoxy and subjected to external pressure, the experimentally determined structural efficiency is 47% greater than that of an all-aluminum cylinder of similar geometry. It is shown that problems involving joints and attachments, which are critical for all-composite structures, are minimized through the use of new design concepts.

Nomenclature

B_x, B_y = extensional stiffness of orthotropic cylinder in axial x and hoop direction y, respectively, lb/in.
D_x, D_y = flexural stiffness of orthotropic cylinder in axial x and hoop y directions, respectively, in.-lb
D_{xy} = twisting stiffness in xy plane, in.-lb
E = modulus of elasticity, psi
G_{xy} = shear stiffness in xy plane, lb/in.
p = external pressure, psi
N_x = axial buckling load, lb/in.
$\hat{\mu}_{xy}$ = relates strain in the y direction due to normal stress in the x direction
$\hat{\mu}_{yx}$ = relates strain in the x direction due to normal stress in the y direction
μ_{xy} = relates strain in the y direction due to flexural stress in the x direction
μ_{yx} = relates strain in the x direction due to flexural stress in the y direction
h = rib height, in.

Presented as Paper 70-101 at the AIAA 8th Aerospace Sciences Meeting, New York, January 19–21, 1970; submitted March 24, 1970; revision received November 5, 1970. The authors wish to express their appreciation to R. J. Nebesar for his assistance during this program and for aiding in the fabrication of test specimens. This work was performed under the sponsorship of the McDonnell Douglas Astronautics Company—West under an independent research and development program.

* Staff Engineer, Advance Structures and Mechanical Department. Member AIAA.
† Engineer/Scientist Specialist, Advance Structures and Mechanical Department. Member AIAA.